Functional Impact of *ZEB1* Mutations Associated With Posterior Polymorphous and Fuchs' Endothelial Corneal Dystrophies

Duk-Won D. Chung, Ricardo F. Frausto, Lydia B. Ann, Michelle S. Jang, and Anthony J. Aldave

The Jules Stein Eye Institute, David Geffen School of Medicine at University of California-Los Angeles, Los Angeles, California, United States

Correspondence: Anthony J. Aldave, The Jules Stein Eye Institute, 100 Stein Plaza, UCLA, Los Angeles, CA 90095-7003, USA; aldave@jsei.ucla.edu.

D-WDC and RFF contributed equally to the work presented here and should therefore be regarded as equivalent authors.

Submitted: July 16, 2014
Accepted: August 26, 2014

Citation: Chung D-WD, Frausto RF, Ann LB, Jang MS, Aldave AJ. Functional impact of *ZEB1* mutations associated with posterior polymorphous and Fuchs' endothelial corneal dystrophies. *Invest Ophthalmol Vis Sci*. 2014;55:6159–6166. DOI: 10.1167/iovs.14-15247

Purpose. To assess the impact of zinc finger E-box binding homeobox 1 (*ZEB1*) gene mutations associated with posterior polymorphous corneal dystrophy 3 (PPCD3) and Fuchs' endothelial corneal dystrophy (FECD).

Methods. Thirteen of the 27 previously reported *ZEB1* truncating mutations associated with PPCD3 and the six previously reported *ZEB1* missense mutations associated with FECD were generated and transiently transfected into a corneal endothelial cell line. Protein abundance was determined by immunoblotting, while intracellular localization was determined by fluorescence confocal microscopy.

Results. Three of the 13 ZEB1 truncated mutants, and none of the missense mutants, showed significant decrease in mutant ZEB1 protein levels. Predominant nuclear localization was observed for truncated ZEB1 mutant proteins with a predicted molecular weight of less than 92 kilodaltons. The two largest mutant proteins that lacked a putative nuclear localization signal (NLS), p.(Ser638Cysfs*5) and p.(Gln884Argfs*37), primarily localized to the cytoplasm, while the NLS-containing mutant proteins, p.(Glu997Alafs*7) and p.(Glu1039Glyfs*6), primarily localized to the nucleus. All the missense ZEB1 mutant proteins were exclusively present in the nucleus.

Conclusions. ZEB1 truncating mutations result in a significant decrease and/or impaired nuclear localization of the encoded protein, indicating that ZEB1 haploinsufficiency in PPCD3 may result from decreased protein production and/or impaired cellular localization. Conversely, as the reported *ZEB1* missense mutations do not significantly impact protein abundance or nuclear localization, the effect of these mutations on ZEB1 function and their relationship to FECD, if any, remain to be elucidated.

Keywords: posterior polymorphous corneal dystrophy, Fuchs' endothelial corneal dystrophy, *ZEB1*, corneal endothelium

In the last 10 years, several genes have been identified through linkage and association studies as playing a role in the development of corneal endothelial dystrophies, including the identification of protein truncating mutations in the zinc finger E-box binding homeobox 1 gene (*ZEB1*) in posterior polymorphous corneal dystrophy linked to chromosome 10 (PPCD3).[1,2] Once identified, these genes serve as attractive candidate genes for other corneal endothelial dystrophies with similar phenotypic features. Thus, screening of *ZEB1* in individuals with Fuchs' endothelial corneal dystrophy (FECD) has led to the identification of a half dozen missense mutations that were predicted to be pathogenic using in silico analysis.[3,4] Krafchak and colleagues[1] were the first to report nonsense and frameshift *ZEB1* mutations as the cause of PPCD3 and identified potential ZEB1 binding sites in the promoter region of the collagen type IV alpha 3 gene (*COL4A3*). Their demonstration of the expression of COL4A3 in the endothelium of an individual with PPCD3, and the absence of expression in a control individual, led to the initial theory of the pathogenesis of PPCD3, that is, that ZEB1 truncating mutations lead to *ZEB1* haploinsufficiency and the loss of ZEB1-mediated inhibition of COL4A3 expression. Krafchak and colleagues[1] hypothesized that this resulted in ectopic COL4A3 expression in the corneal endothelium and the subsequent development of PPCD, although we subsequently demonstrated COL4A3 expression in healthy human corneal endothelial cells.[5] However, what effect these *ZEB1* mutations have on the production and function of the encoded ZEB1 protein, and thus the mechanisms by which the *ZEB1* mutations result in the loss of regulatory inhibition of COL4A3, have not been investigated. In addition, no functional studies have been performed to investigate the effect of the identified ZEB1 truncating and missense mutations on the production and function of the encoded protein. Therefore, we transfected a corneal endothelial cell line with DNA constructs containing *ZEB1* cDNA corresponding to the ZEB1 truncating mutations that we have reported in individuals with PPCD,[6,7] as well as with ZEB1 missense mutations identified in individuals with FECD, to determine the effect of these mutations on the production and intracellular localization of the mutant ZEB1 proteins.

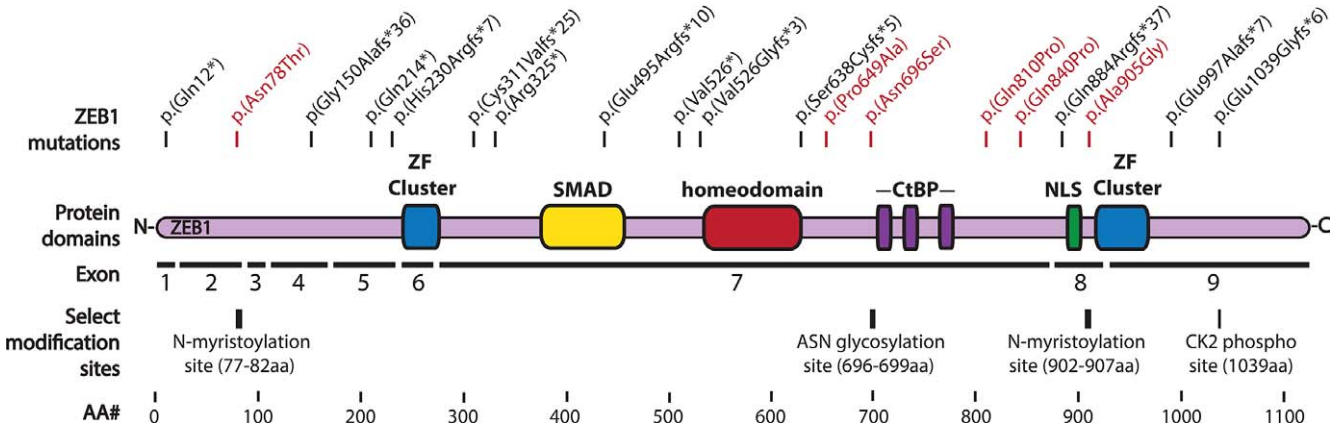

Figure 1. Depiction of the ZEB1 protein. ZEB1 truncating mutations are shown in *black font*, and ZEB1 missense mutations are shown in *red font*. Predicted ZEB1 protein domains and modification sites that overlap with reported ZEB1 mutations are shown. ZF, zinc finger; NLS, nuclear localization signal; CtBP, C-terminal binding protein.

Methods

ZEB1 Mutagenesis and Plasmid Constructs

We created mutant constructs corresponding to 13 of the 14 truncating mutations in *ZEB1* that we have previously reported (Fig. 1; Table 1).[6,7] We excluded the p.(Met1?) mutant as it was predicted to either not express a protein or express one not resembling ZEB1. These 14 mutations, which represent approximately half of the 27 mutations associated with PPCD3, are present in six of the nine coding exons of *ZEB1*, and are located in the same exons as the other 13 reported *ZEB1* truncating mutations (Fig. 1).[1,8–12] In addition, we created mutant constructs corresponding to the six previously reported ZEB1 missense mutations associated with FECD (Fig. 1; Table 2). All mutant constructs were generated using mutation-specific primers (Supplementary Table S1) and the Phusion Site-Directed Mutagenesis kit (Thermo Fisher Scientific, Waltham, MA, USA). Each mutation was introduced into a commercially available pReceiver-M49(a,x,y) expression vector (GeneCopoeia, Rockville, MD, USA) containing $ZEB1^{WT}$ variant 2 cDNA (National Center for Biotechnology Information [NCBI] accession no. NM_030751.5) downstream of the HaloTag sequence. $ZEB1^{MU}$ DNA constructs were generated and purified using PerfectPrep Spin Mini Kit (5 PRIME; Fisher Scientific, Pittsburgh, PA, USA) and HiPure Plasmid Filter Maxiprep kit (Life Technologies, Grand Island, NY, USA). We confirmed the presence of each mutation by Sanger sequencing.

Cell Culture and Transfection

Experiments were performed in HCEnC-21T cells, a telomerase immortalized human corneal endothelial cell line.[13] Cells were grown on cell culture grade plastic coated with 40 μg/cm^2 chondroitin sulfate A (Sigma-Aldrich Corp., St. Louis, MO, USA) and 40 ng/cm^2 laminin (Sigma-Aldrich Corp.) in phosphate-buffered saline (PBS) for 2 hours. Cells were incubated at 37°C in 5% CO_2 in medium containing a 1:1 ratio of F10-Ham's medium and M199 medium (Life Technologies) supplemented with 5% (vol/vol) fetal bovine serum (Atlanta Biologicals, Flowery Branch, GA, USA), 20 μg/mL ascorbic acid (Sigma-Aldrich Corp.), 20 μg/mL insulin (Life Technologies), 10 μg/mL bFGF (PeproTech, Inc., Rocky Hill, NJ, USA), and 100 U/mL penicillin and 100 ug/mL streptomycin (Life Technologies). DNA was transiently transfected into HCEnC-21T cells using Lipofectamine LTX (Life Technologies) reagent according to manufacturer's instructions. As a negative control, transfection using empty pCMV6-Entry vector (Or-

Table 1. Summary of Immunoblotting Results for PPCD3 Truncating Mutations

ZEB1 Protein	Predicted MW, kDa, Without Halo-Tag	Predicted MW, kDa, With Halo-Tag	Measured MW, kDa	Protein Abundance vs. $ZEB1^{WT}$, Ratio
$ZEB1^{WT}$	124	157	161	1.00
p.(Gln12*)	2	35	37	1.21
p.(Gly150fs)	21	54	60	0.76
p.(Gln214*)	24	57	63	1.2
p.(His230fs)	27	60	65	1.03
p.(Cys311fs)	38	71	73	0.38
p.(Arg325*)	37	70	72	1.07
p.(Glu495fs)	56	89	91	0.63
p.(Val526*)	58	91	93	0.42
p.(Val526fs)	58	91	91	0.1
p.(Ser638fs)	71	104	104	0.99
p.(Gln884fs)	101	134	139	0.05
p.(Glu997fs)	110	143	148	0.05
p.(Glu1039fs)	115	148	155	0.93

The HaloTag adds approximately 33 kDa to the MW of each ZEB1 protein.

Investigative Ophthalmology & Visual Science

Table 2. In Silico Analysis of ZEB1 Missense Mutations Associated With FECD

ZEB1 Mutation	Polyphen-2 Probability Score & Prediction	SIFT Score & Prediction	Predicted Modification Sites That Overlap With FECD Mutations*
p.(Asn78Thr)	0.013 Benign	0.08 Tolerated	N-myristoylation
p.(Pro649Ala)	0.104 Benign	0.11 Tolerated	None
p.(Asn696Ser)	0.087 Benign	0.22 Tolerated	Asn-glycosylation, N-myristoylation
p.(Gln810Pro)	0.996 Probably damaging	0.18 Tolerated	None
p.(Gln840Pro)	0.996 Probably damaging	0.14 Tolerated	None
p.(Ala905Gly)	0.997 Probably damaging	0.01 Damaging	N-myristoylation

* PredictProtein was used for the identification of protein modification sites.

igene Technologies, Rockville, MD, USA) was also performed. Cotransfection with pcDNA3.1-*GFP* was performed to control for transfection efficiency.

Protein Abundance Analysis

HaloTag-*ZEB1*^{WT} and HaloTag-*ZEB1*^{MU} constructs were transiently transfected into HCEnC-21T cells, and HaloTag-ZEB1 protein levels were analyzed by immunoblotting with an anti-HaloTag antibody (Promega, Madison, WI, USA). Whole cell lysates were prepared using modified-radioimmunoprecipitation assay (RIPA) lysis buffer containing phosphatase and protease inhibitors. Five micrograms of total protein was subjected to sodium dodecyl sulfate–polyacrylamide gel electrophoresis (SDS-PAGE) and subsequently transferred onto a 0.45-μm polyvinylidene fluoride membrane. HaloTag-ZEB1 proteins were detected using a polyclonal anti-HaloTag antibody (Promega) at 1:2000 dilution in Tris-buffered saline, Tween 20 (TBST) containing 5% skim milk. Immunoblotting for α-tubulin was performed as a loading control using an anti-α-tubulin (TUBA) antibody (Cell Signaling, Boston, MA, USA) at 1:4000. As a control for transfection efficiency, green fluorescent protein (GFP) was detected with a monoclonal anti-GFP antibody (Life Technologies). Secondary antibodies (Millipore, Billerica, MA, USA) conjugated to horseradish peroxidase (HRP) were used at a dilution factor of 1:30,000. Chemiluminesence was performed using the Luminata Forte HRP substrate (Millipore), and luminescence was exposed to Hyperfilm (GE Healthcare Bio-Sciences, Pittsburgh, PA, USA) followed by densitometric analysis by ImageJ software.[14]

Protein Localization Analysis

HaloTag-*ZEB1*^{WT} and HaloTag-*ZEB1*^{MU} DNA constructs were transiently transfected into HCEnC-21T cells grown on laminin-coated (40 ng/cm^2) coverslips. Cells were fixed in 4% paraformaldehyde (PFA) solution in PBS and permeabilized in 0.25% Triton X-100, then washed with ice-cold PBS and blocked with PBST (PBS + 0.05% Tween 20) containing 1% BSA and 10% normal goat serum (NGS). HaloTag-ZEB1 was detected with rabbit anti-HaloTag primary antibody (Promega), which was diluted 1:1000 in blocking solution and incubated overnight at 4°C. Cells were washed with PBST three times and then incubated with an anti-rabbit Alexa Fluor 594 (Life Technologies) secondary antibody diluted 1:500 in blocking buffer for 1 hour at room temperature. Cells were washed with PBST three times and subsequently mounted with DAPI (4′,6-diamidino-2-phenylindole) containing aqueous mounting medium (Vectashield H1200; Vector Laboratories, Burlingame, CA, USA). Fluorescence was imaged using confocal microscopy, and the nuclear-to-cytoplasmic fluorescence ratio was calculated from the measured fluorescence per pixel value obtained from a selected region of interest within the nucleus and cytoplasm for the ZEB1^{WT} and ZEB1^{MU} proteins.

In Silico Protein Analysis of ZEB1

The NCBI Entrez query and the Conserved Domain Database (CDD) were utilized to determine the presence and location of putative ZEB1 functional and DNA binding domains.[15] The amino acid sequence for ZEB1, isoform b (NCBI Reference Sequence: NP_110378.3), was input into PredictProtein (www.predictprotein.org [in the public domain]) in order to identify putative binding domains and modification sites.[16,17] PolyPhen-2 (v2.2.2r398) and SIFT algorithms were used to predict the effect of the ZEB1 missense mutations that have been associated with FECD.[18,19]

Statistical Analyses

Protein abundance was statistically analyzed using one-way ANOVA with Dunnett's multiple comparison test within GraphPad Prism software (GraphPad Software, La Jolla, CA, USA).

Results

Selected ZEB1 Truncating Mutations Are Associated With Significant Reduction in the Corresponding ZEB1 Protein

To determine the impact of ZEB1 truncating mutations on the expression of ZEB1 protein, HCEnC-21T cells were transiently transfected with HaloTag-*ZEB1* DNA constructs. Immunoblotting for the HaloTag demonstrated a statistically significant decrease in abundance of 3 of the 13 ZEB1^{MU} proteins [p.(Val526fs), p.(Gln884fs), and p.(Glu997fs)] compared with ZEB1^{WT} (Fig. 2; Table 1). The abundance of ZEB1^{MU} proteins containing a deletion (nuclear localizaton signal [NLS]del) or alteration (NLS Lys>Ile and NLS Lys>Ala) of the putative NLS sequence did not differ significantly from ZEB1^{WT} protein levels.

Selected ZEB1 Truncating Mutations Are Associated With Altered Nuclear Localization

Immunofluorescence confocal imaging was performed on HCEnC-21T cells transiently transfected with HaloTag-*ZEB1*^{WT} or HaloTag-*ZEB1*^{MU} constructs (Figs. 3, 4). As expected for a transcription factor such as ZEB1 that must localize to the nucleus to regulate protein expression, ZEB1^{WT} protein demonstrated exclusive nuclear localization. While ZEB1^{MU} proteins with a predicted molecular weight equal to or less than 58 kDa (92 kDa with HaloTag) were primarily localized to

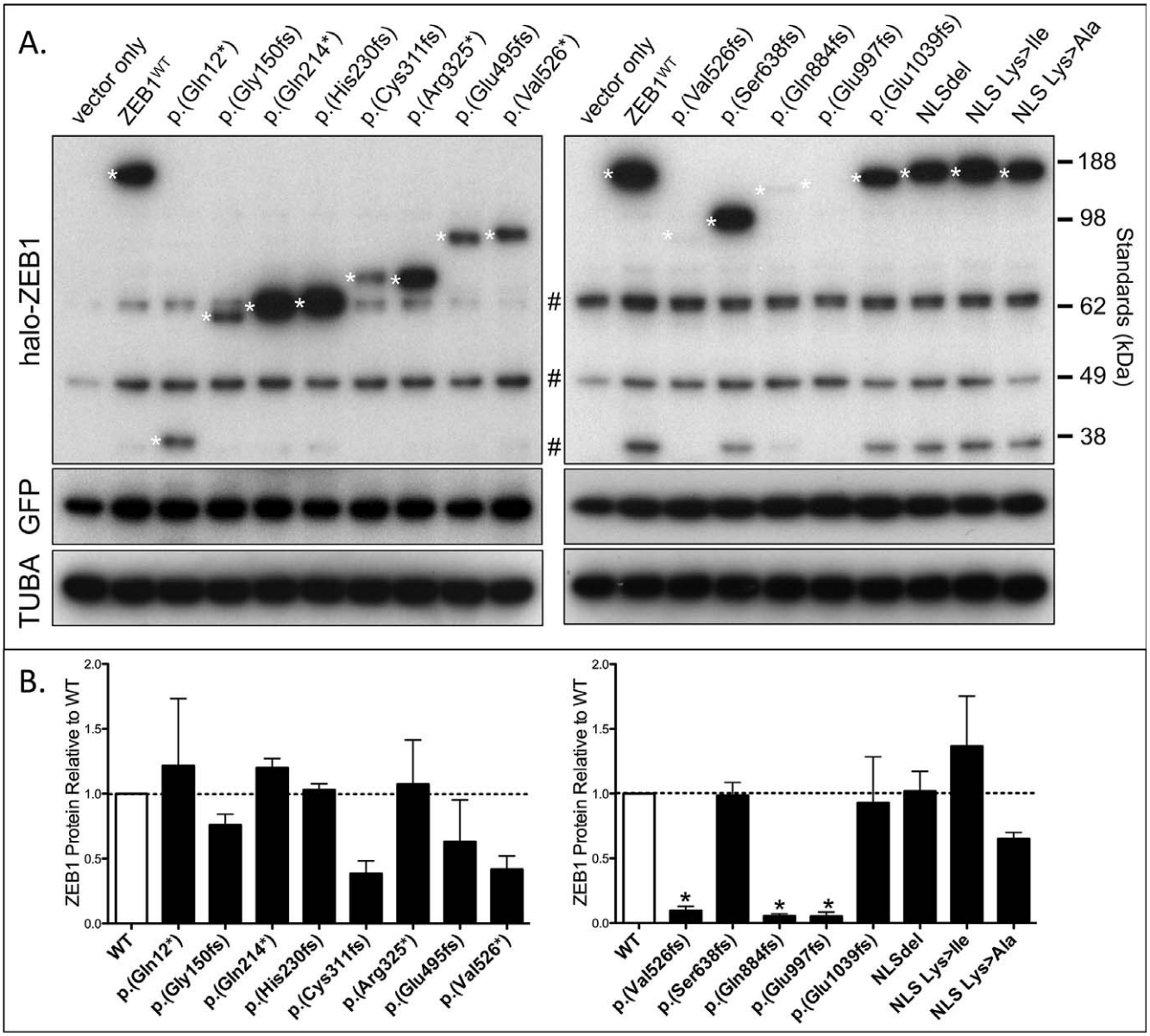

Figure 2. Quantification of ZEB1 mutant proteins associated with PPCD3. HCEnC-21T cells were cotransfected with HaloTag-*ZEB1*^{WT} or nonsense HaloTag-*ZEB1*^{MU} together with a GFP construct. (**A**) Protein lysates were subjected to SDS-PAGE, and immunoblotting for the HaloTag, GFP, and TUBA was performed. NLS, nuclear localization signal. *Number sign* denotes nonspecific bands. *White asterisks* denote proteins with HaloTag. (**B**) Protein abundance was compared to ZEB1^{WT} protein, normalized for transfection efficiency (GFP) and loading (TUBA), and plotted as a ratio of ZEB1^{MU} to ZEB1^{WT}. *Black asterisks* denote ZEB1^{MU} protein levels that are statistically different from ZEB1^{WT} levels ($P < 0.05$, $n = 3$, *error bars* = SEM).

the nucleus, weak and diffuse localization in the cytoplasm was also observed. ZEB1^{MU} proteins just larger than 58 kDa, such as p.(Cys311Valfs*25) and p.(Arg325*), were exclusively localized to the nucleus. In contrast, the p.(Ser638fs) and p.(Gln884fs) ZEB1^{MU} proteins were primarily localized to the cytoplasm, presumably due to size exclusion from the nucleus and absence of a putative PKKKMRK nuclear localization signal, predicted using protein landscape prediction tools to be at residue 892 in exon 8. ZEB1^{MU} proteins with an intact putative NLS sequence, p.(Glu997fs) and p.(Glu1039fs), were primarily localized to the nucleus. Transient transfection with a *ZEB1*^{MU} construct with a deleted or altered putative NLS (NLSdel, NLS Lys>Ile and NLS Lys>Ala) demonstrated exclusive cytoplasmic localization.

ZEB1 Missense Mutations Are Not Associated With Significant Changes in ZEB1 Protein Abundance

To determine the impact of ZEB1 missense mutations on ZEB1 protein production and cellular localization, HCEnC-21T cells were transfected with the HaloTag-*ZEB1*^{WT} and a set of HaloTag-*ZEB1*^{MU} constructs comprising each of the six ZEB1 missense mutations associated with FECD. Immunoblotting for the HaloTag demonstrated that the missense mutations did not alter ZEB1 protein production when compared with ZEB1^{WT} protein levels (Fig. 5).

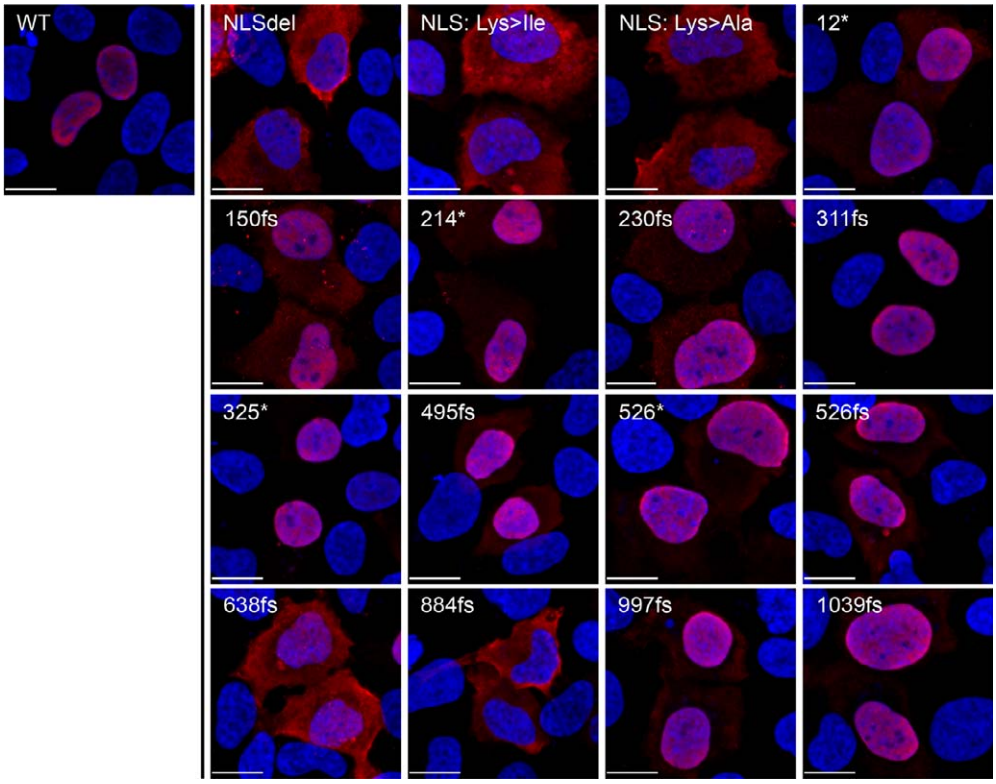

Figure 3. Cellular localization of ZEB1 mutant proteins associated with PPCD3. Truncated ZEB1 mutant proteins (*red*) with a predicted molecular weight equal to or less than 58 kDa (91 kDa with HaloTag) primarily localized to the nucleus but also showed diffused cytoplasmic localization, whereas ZEB1^{WT} protein was exclusively in the nucleus. The p.(Ser638fs) and p.(Gln884fs) proteins were primarily localized to the cytoplasm due to size exclusion from the nucleus and absence of the putative nuclear localization signal (NLS). With an intact putative NLS sequence, the p.(Glu997fs) and p.(Glu1039fs) mutants were primarily localized to the nucleus. Nuclei were stained with DAPI (*blue*). *Scale bars*: 15 μm.

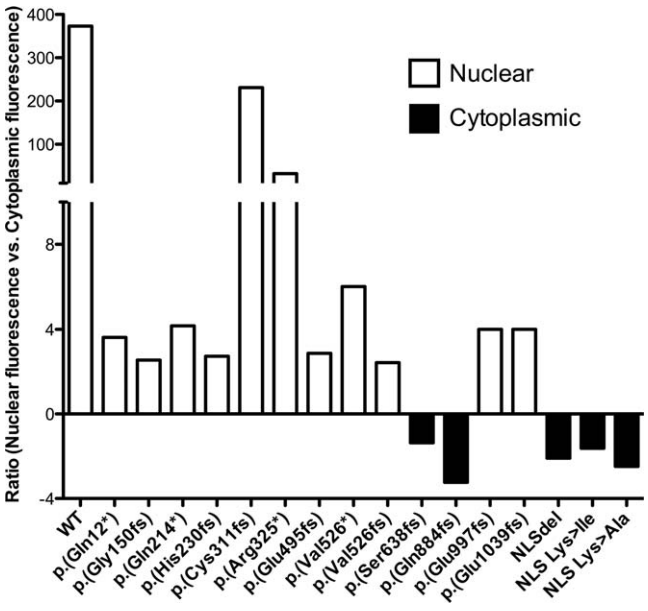

Figure 4. Relative quantification of ZEB1 mutant proteins associated with PPCD in the nucleus and cytoplasm. A ratio was calculated from the measured fluorescence per pixel value obtained from a selected region of interest within the nucleus and cytoplasm for the ZEB1^{WT} and ZEB1^{MU} proteins. The mutants in between and including p.(Cys311fs) and p.(Val526fs) were localized primarily in the nucleus, with p.(Cys311fs) and p.(Arg325*) strongly resembling the results obtained with the ZEB1^{WT} protein.

ZEB1 Missense Mutations Are Not Associated With Altered Nuclear Localization

Immunofluorescence confocal imaging of HCEnC-21T cells transiently transfected with HaloTag-*ZEB1*^{WT} and HaloTag-*ZEB1*^{MU} constructs revealed that each ZEB1^{MU} protein corresponding to a missense mutation demonstrated exclusive nuclear localization, similar to the ZEB1^{WT} protein (Fig. 6).

FECD-Associated ZEB1 Missense Mutations Coincide With Predicted Protein Modification Sites

Using the PredictProtein server, we identified putative protein modification sites within ZEB1, several of which coincide with the amino acid residues at which missense mutations associated with FECD have been identified (Fig. 1; Table 2). Polyphen-2 predicted p.(Gln810Pro), p.(Gln840Pro), and p.(Ala905Gly) to be probably damaging while SIFT predicted only p.(Ala905Gly) to be deleterious (Table 2).

Discussion

ZEB1 is integrally involved in epithelial-to-mesenchymal transition (EMT) and plays critical roles in both development (e.g., embryonic gastrulation) and disease (e.g., tumorigenesis) by repressing the transcription of genes important in maintaining the epithelial phenotype.[20–23] ZEB1 has been shown to repress the transcription of a variety of genes, including several involved in EMT.[24–27] The role of ZEB1 in corneal endothelial cell function remains unknown, but the identification of *ZEB1* mutations associated with corneal

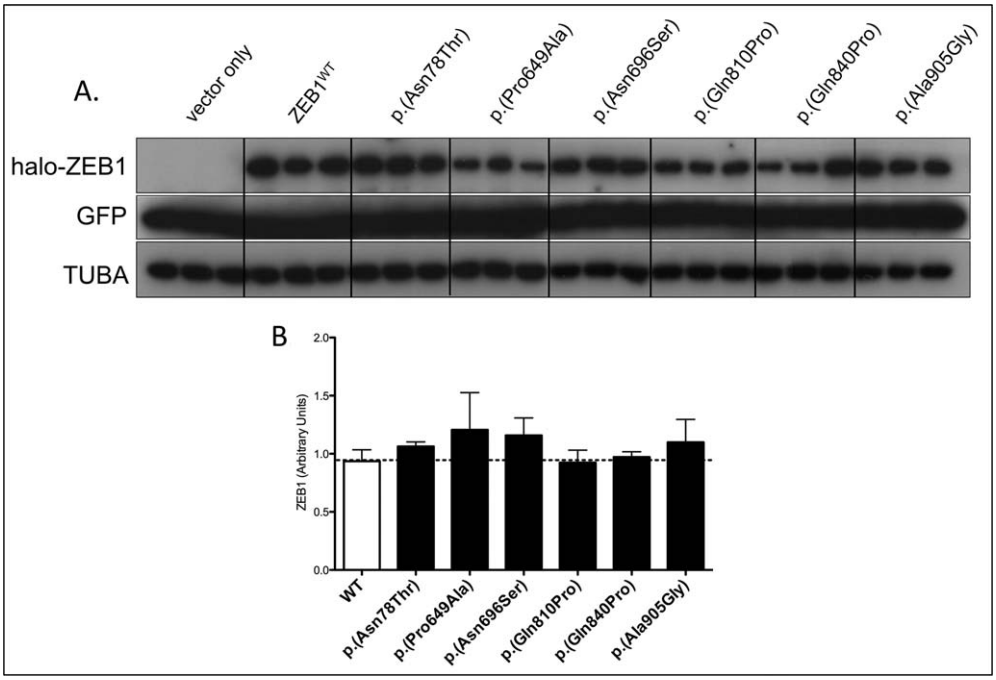

Figure 5. Quantification of ZEB1 mutant proteins associated with FECD. HCEnC-21T cells were cotransfected with HaloTag-*ZEB1*^{WT} or missense HaloTag-*ZEB1*^{MU} together with a GFP construct. (**A**) Protein lysates were subjected to SDS-PAGE, and immunoblotting for the HaloTag, GFP, and TUBA was performed. (**B**) Protein abundance was compared to ZEB1^{WT} protein, normalized for transfection efficiency (GFP) and loading (TUBA), and plotted as a ratio of ZEB1^{MU} to ZEB1^{WT}. None of the six FECD-associated missense mutations exhibited significant protein abundance changes.

endothelial dystrophies provides evidence that the ZEB1 protein plays an important role in maintaining endothelial cell function and corneal clarity. All 27 reported PPCD3 mutations result in the generation of a premature stop codon, which is predicted to both lead to the truncation of the ZEB1 protein and result in *ZEB1* haploinsufficiency.[1,6–10] The six *ZEB1* mutations associated with FECD are missense mutations found at either highly or moderately conserved sites; and it has been suggested that these ZEB1 missense mutations are hypomorphic, inducing a less severe pathogenic phenotype compared to PPCD.[3,4] Our aim in analyzing the 13 PPCD3-associated and six FECD-associated *ZEB1* mutations was to gain insight into how specific *ZEB1* mutations lead to the distinct disease phenotypes characteristic of PPCD3 and FECD.

Although the consensus is that mutations that truncate ZEB1 lead to haploinsufficiency and result in PPCD3, there is a paucity of experimental evidence supporting this hypothesis. With an approach combining protein abundance and localization studies, our data suggest that PPCD3 develops as a consequence of truncating mutations that hinder ZEB1 function by various mechanisms, including the deletion of vital functional domains, decreased protein abundance, and/or improper cellular localization.

As the first group to confirm ZEB1 nuclear localization in endothelium of ex vivo corneal tissue and primary corneal

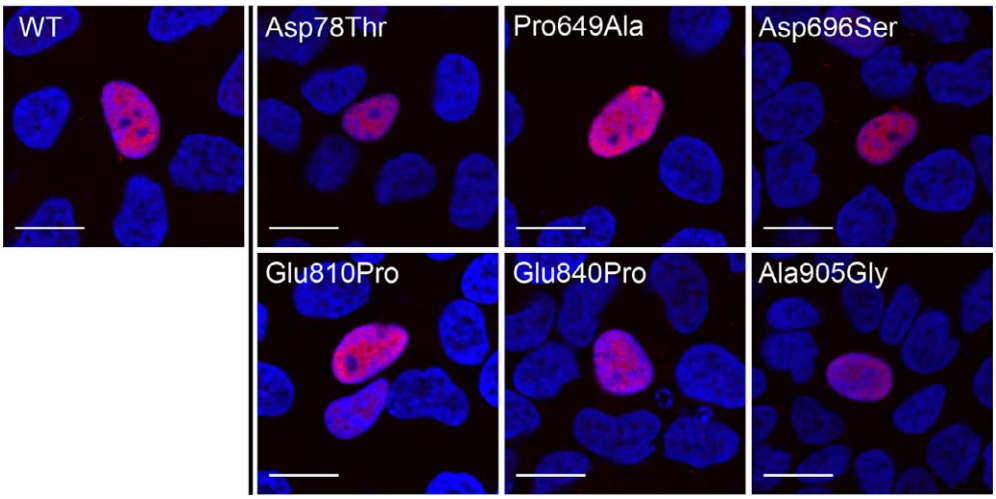

Figure 6. Cellular localization of ZEB1 mutant proteins associated with FECD. Fuchs' endothelial corneal dystrophy–associated ZEB1 missense mutations did not affect cellular localization. All six ZEB1 missense proteins (*red*) properly localized to the nucleus. Nuclei were stained with DAPI (*blue*). *Scale bars*: 15 μm.

endothelial cells, we also now have identified and confirmed the existence of the ZEB1 NLS, which we show is sufficient and necessary for nuclear import of ZEB1.[5,28] The ZEB1 mutations p.(Ser638Cysfs*5) and p.(Gln884Argfs*37) are expected to have intact homeodomains, with p.(Ser638-Cysfs*5) having no observed reduction in protein abundance. The observation that these two mutant proteins were exclusively cytoplasmic can be explained by the fact that they lack the NLS and are well above the threshold for simple diffusion into the nucleus (approximately 60 kD).[29] Thus, p.(Ser638Cysfs*5) and p.(Gln884Argfs*37) likely lead to haploinsufficiency by abrogating nuclear translocation and not allowing ZEB1 to regulate gene transcription. Although the exon 7 mutants p.(Cys311Valfs*25), p.(Arg325*), p.(Glu495Argfs*10), and p.(Val526*) also lack the putative NLS located in exon 8 and are predicted to be too large to passively diffuse across the nuclear pores, these mutant proteins localized primarily to the nucleus. We hypothesize that an alternative NLS motif (Lys-Lys-Arg) located at residues 274 to 276 is unmasked by the ZEB1 truncating mutations, thus allowing for the active transport across the nuclear envelope.

Our results show that ZEB1 truncating mutations can lead to a significant decrease in protein abundance compared with $ZEB1^{WT}$, as was observed with p.(Val526*), p.(Gln884Argfs*37), and p.(Glu997Alafs*7). This observed decrease in ZEB1 protein levels is likely the result of nonsense-mediated decay, which has been previously reported to cause haploinsufficiency in various heritable disorders associated with heterozygous mutations that lead to an early stop codon.[30–33]

The p.(Glu1039Glyfs*6) mutation did not show altered protein production or cellular localization. In addition, all of the well-characterized ZEB1 protein domains (zinc finger, homeodomain, CtBP binding site, and SMAD interacting domain) are retained.[34,35] In spite of this, the mutant protein does lack the 86 C-terminal amino acids, which may harbor putative functional domains important to ZEB1 function. Our in silico protein analysis identified a putative casein kinase 2 (CK2) phosphorylation site at residues 1036 to 1039. Casein kinase 2 activity is closely linked to the Wnt/β-catenin signaling pathway, which is implicated in various cellular processes including cell fate determination and cell proliferation.[36] Though validation has yet to be performed, perhaps the loss of this putative CK2 phosphorylation site causes the inactivity, and subsequent haploinsufficiency, of ZEB1 in PPCD3.

Lacking the primary putative NLS but still capable of translocating across the nuclear pores, either by simple diffusion or with the aid of an alternative putative NLS, ZEB1 truncating mutations p.(Gln12*), p(Gly150Alafs*36), p.(Gln214*), p.(His230Argfs*7), p.(Cys311Valfs*25), p.(Arg325*), p.(Glu495Argfs*10), and p.(Val526*) demonstrate primarily nuclear localization without a statistically significant decrease in protein abundance. Therefore, these mutations must mediate their effects on ZEB1 function by means other than those investigated in this study. Potential mechanisms via which these mutations may impact ZEB1 function and lead to PPCD3 are suggested by identification of both the well-characterized and putative functional domains in ZEB1 using NCBI's Entrez query and the CDD (Fig. 1). In general, we expect the truncation mutations that occur prior to amino acid residues 581 to 629 to result in the loss of the ZEB1 homeodomain and the C-terminal zinc finger cluster, which are integral to ZEB1's DNA binding properties.[15,37] ZEB1 contains two zinc finger domain clusters, located at amino acids 240 to 277 and 918 to 971. It has been previously shown that multiple zinc finger domains in transcription factors can work in concert in order to bind to DNA.[38] Thus, for ZEB1 truncating mutations that remove the C-terminal zinc finger cluster or the most C-terminal zinc finger domain, it is plausible that a loss of DNA binding activity is due to an inability of the two zinc finger clusters to act in concert.[39]

Although the data that we present do not indicate a mechanism whereby the identified ZEB1 missense mutations associated with FECD lead to impairment of ZEB1 production or function, we can state that they do not appear to affect ZEB1 protein production or nuclear localization. Additionally, none of the FECD missense mutations was located in a well-characterized functional domain of ZEB1, effectively excluding dysfunction of one of these domains caused by a missense mutation. However, an in silico ZEB1 protein analysis to identify other putative or unknown functional domains present in ZEB1 revealed that three of the six ZEB1 missense mutations associated with FECD are found within putative ZEB1 regulatory or modification sites (Table 2). In addition, two of the other three ZEB1 missense mutations are located within a predicted myristoylation or glycosylation site; these have been implicated in a wide array of roles that include protein regulation and signaling (Fig. 1).[40–42] Although Riazuddin and colleagues[4] reported that both SIFT and PolyPhen predicted that each of the five ZEB1 missense mutations they associated with FECD was pathogenic, we found that only p.(Ala905Gly) was predicted to be damaging by both programs.

All together, our data suggest that PPCD3 is caused by *ZEB1* haploinsufficiency as a result of nonfunctional ZEB1, as a consequence of either the loss of functional domains or dysfunction in the regulation and activity of mutant ZEB1. In contrast, we were not able to identify an effect of the missense mutations previously identified in FECD patients on ZEB1 protein expression or nuclear localization, although in silico analyses indicate that the mutations may alter putative ZEB1 regulatory or modification sites.

Acknowledgments

The authors thank Jonathan Han and Cynthia Wang for their technical assistance in generating *ZEB1* mutant constructs.

Supported by National Eye Institute Grants 1R01 EY022082 (AJA) and P30 EY000331 (Core Grant) and an unrestricted grant from Research to Prevent Blindness.

Disclosure: **D.-W.D. Chung**, None; **R.F. Frausto**, None; **L.B. Ann**, None; **M.S. Jang**, None; **A.J. Aldave**, None

References

1. Krafchak CM, Pawar H, Moroi SE, et al. Mutations in TCF8 cause posterior polymorphous corneal dystrophy and ectopic expression of COL4A3 by corneal endothelial cells. *Am J Hum Genet*. 2005;77:694–708.
2. Schmedt T, Silva MM, Ziaei A, Jurkunas U. Molecular bases of corneal endothelial dystrophies. *Exp Eye Res*. 2012;95:24–34.
3. Mehta JS, Vithana EN, Tan DT, et al. Analysis of the posterior polymorphous corneal dystrophy 3 gene, TCF8, in late-onset Fuchs endothelial corneal dystrophy. *Invest Ophthalmol Vis Sci*. 2008;49:184–188.
4. Riazuddin SA, Zaghloul NA, Al-Saif A, et al. Missense mutations in TCF8 cause late-onset Fuchs corneal dystrophy and interact with FCD4 on chromosome 9p. *Am J Hum Genet*. 2010;86:45–53.
5. Yellore VS, Rayner SA, Nguyen CK, et al. Analysis of the role of ZEB1 in the pathogenesis of posterior polymorphous corneal dystrophy. *Invest Ophthalmol Vis Sci*. 2012;53:273–278.
6. Aldave AJ, Yellore VS, Yu F, et al. Posterior polymorphous corneal dystrophy is associated with TCF8 gene mutations and abdominal hernia. *Am J Med Genet A*. 2007;143A:2549–2556.

7. Bakhtiari P, Frausto RF, Roldan AN, Wang C, Yu F, Aldave AJ. Exclusion of pathogenic promoter region variants and identification of novel nonsense mutations in the zinc finger E-box binding homeobox 1 gene in posterior polymorphous corneal dystrophy. *Mol Vis*. 2013;19:575–580.
8. Liskova P, Tuft SJ, Gwilliam R, et al. Novel mutations in the ZEB1 gene identified in Czech and British patients with posterior polymorphous corneal dystrophy. *Hum Mutat*. 2007;28:638.
9. Vincent AL, Niederer RL, Richards A, Karolyi B, Patel DV, McGhee CN. Phenotypic characterisation and ZEB1 mutational analysis in posterior polymorphous corneal dystrophy in a New Zealand population. *Mol Vis*. 2009;15:2544–2553.
10. Nguyen DQ, Hosseini M, Billingsley G, Heon E, Churchill AJ. Clinical phenotype of posterior polymorphous corneal dystrophy in a family with a novel ZEB1 mutation. *Acta Ophthalmol*. 2010;88:695–699.
11. Liskova P, Palos M, Hardcastle AJ, Vincent AL. Further genetic and clinical insights of posterior polymorphous corneal dystrophy 3. *JAMA Ophthalmol*. 2013;131:1296–1303.
12. Lechner J, Dash DP, Muszynska D, et al. Mutational spectrum of the ZEB1 gene in corneal dystrophies supports a genotype-phenotype correlation. *Invest Ophthalmol Vis Sci*. 2013;54:3215–3223.
13. Schmedt T, Chen Y, Nguyen TT, Li S, Bonanno JA, Jurkunas UV. Telomerase immortalization of human corneal endothelial cells yields functional hexagonal monolayers. *PLoS One*. 2012;7:e51427.
14. Schneider CA, Rasband WS, Eliceiri KW. NIH Image to ImageJ: 25 years of image analysis. *Nat Methods*. 2012;9:671–675.
15. Marchler-Bauer A, Zheng C, Chitsaz F, et al. CDD: conserved domains and protein three-dimensional structure. *Nucleic Acids Res*. 2013;41:D348–D352.
16. Cokol M, Nair R, Rost B. Finding nuclear localization signals. *EMBO Rep*. 2000;1:411–415.
17. Rost B, Yachdav G, Liu J. The PredictProtein server. *Nucleic Acids Res*. 2004;32:W321–W326.
18. Kumar P, Henikoff S, Ng PC. Predicting the effects of coding non-synonymous variants on protein function using the SIFT algorithm. *Nat Protoc*. 2009;4:1073–1081.
19. Adzhubei IA, Schmidt S, Peshkin L, et al. A method and server for predicting damaging missense mutations. *Nat Methods*. 2010;7:248–249.
20. Park SM, Gaur AB, Lengyel E, Peter ME. The miR-200 family determines the epithelial phenotype of cancer cells by targeting the E-cadherin repressors ZEB1 and ZEB2. *Genes Dev*. 2008;22:894–907.
21. Vandewalle C, Van Roy F, Berx G. The role of the ZEB family of transcription factors in development and disease. *Cell Mol Life Sci*. 2009;66:773–787.
22. Gemmill RM, Roche J, Potiron VA, et al. ZEB1-responsive genes in non-small cell lung cancer. *Cancer Lett*. 2011;300:66–78.
23. Li XL, Hara T, Choi Y, et al. A p21-ZEB1 complex inhibits epithelial-mesenchymal transition through the microRNA 183-96-182 cluster. *Mol Cell Biol*. 2014;34:533–550.
24. Murray D, Precht P, Balakir R, Horton WE Jr. The transcription factor deltaEF1 is inversely expressed with type II collagen mRNA and can repress Col2a1 promoter activity in transfected chondrocytes. *J Biol Chem*. 2000;275:3610–3618.
25. Aigner K, Dampier B, Descovich L, et al. The transcription factor ZEB1 (deltaEF1) promotes tumour cell dedifferentiation by repressing master regulators of epithelial polarity. *Oncogene*. 2007;26:6979–6988.
26. Liu Y, Peng X, Tan J, Darling DS, Kaplan HJ, Dean DC. Zeb1 mutant mice as a model of posterior corneal dystrophy. *Invest Ophthalmol Vis Sci*. 2008;49:1843–1849.
27. Kurahara H, Takao S, Maemura K, et al. Epithelial-mesenchymal transition and mesenchymal-epithelial transition via regulation of ZEB-1 and ZEB-2 expression in pancreatic cancer. *J Surg Oncol*. 2012;105:655–661.
28. Aldave AJ, Ann LB, Frausto RF, Nguyen CK, Yu F, Raber IM. Classification of posterior polymorphous corneal dystrophy as a corneal ectatic disorder following confirmation of associated significant corneal steepening. *JAMA Ophthalmol*. 2013;131:1583–1590.
29. Wei X, Henke VG, Strubing C, Brown EB, Clapham DE. Real-time imaging of nuclear permeation by EGFP in single intact cells. *Biophys J*. 2003;84:1317–1327.
30. Lemmens R, Maugeri A, Niessen HW, et al. Novel COL4A1 mutations cause cerebral small vessel disease by haploinsufficiency. *Hum Mol Genet*. 2013;22:391–397.
31. Micale L, Augello B, Maffeo C, et al. Molecular analysis, pathogenic mechanisms, and readthrough therapy on a large cohort of Kabuki syndrome patients. *Hum Mutat*. 2014;35:841–850.
32. Suzuki S, Nakao A, Sarhat AR, et al. A case of pancreatic agenesis and congenital heart defects with a novel GATA6 nonsense mutation: evidence of haploinsufficiency due to nonsense-mediated mRNA decay. *Am J Med Genet A*. 2014;164A:476–479.
33. Konno T, Tada M, Ikeuchi T, et al. Haploinsufficiency of CSF-1R and clinicopathologic characterization in patients with HDLS. *Neurology*. 2014;82:139–148.
34. Zhao LJ, Kuppuswamy M, Vijayalingam S, Chinnadurai G. Interaction of ZEB and histone deacetylase with the PLDLS-binding cleft region of monomeric C-terminal binding protein 2. *BMC Mol Biol*. 2009;10:89.
35. Nakahata S, Yamazaki S, Nakauchi H, Morishita K. Downregulation of ZEB1 and overexpression of Smad7 contribute to resistance to TGF-beta1-mediated growth suppression in adult T-cell leukemia/lymphoma. *Oncogene*. 2010;29:4157–4169.
36. Gao Y, Wang HY. Casein kinase 2 is activated and essential for Wnt/beta-catenin signaling. *J Biol Chem*. 2006;281:18394–18400.
37. Kissinger CR, Liu BS, Martin-Blanco E, Kornberg TB, Pabo CO. Crystal structure of an engrailed homeodomain-DNA complex at 2.8 A resolution: a framework for understanding homeodomain-DNA interactions. *Cell*. 1990;63:579–590.
38. Marco E, Garcia-Nieto R, Gago F. Assessment by molecular dynamics simulations of the structural determinants of DNA-binding specificity for transcription factor Sp1. *J Mol Biol*. 2003;328:9–32.
39. Remacle JE, Kraft H, Lerchner W, et al. New mode of DNA binding of multi-zinc finger transcription factors: deltaEF1 family members bind with two hands to two target sites. *EMBO J*. 1999;18:5073–5084.
40. Legrand P, Rioux V. The complex and important cellular and metabolic functions of saturated fatty acids. *Lipids*. 2010;45:941–946.
41. Scott K, Gadomski T, Kozicz T, Morava E. Congenital disorders of glycosylation: new defects and still counting. *J Inherit Metab Dis*. 2014;37:609–617.
42. Legrain P, Rain JC. Twenty years of protein interactions studies for biological functions deciphering. *J Proteomics*. 2014;107:93–97.

Investigative Ophthalmology & Visual Science